Nanoparticle−Mirror Sandwich Substrates for Surface-Enhanced Raman Scattering

Jacquitta K. Daniels and George Chumanov*

Department of Chemistry, Clemson University, Clemson, South Carolina 29634

Received: June 24, 2005; In Final Form: August 2, 2005

Sandwich surface-enhanced Raman scattering (SERS) substrates (3S) utilizing coupling between continuous metal films and plasmonic particles were fabricated using silver mirrors, electrochemically roughened films, and various sizes of silver nanoparticles. The effect of excitation wavelength and nanoparticle size on SERS spectra of poly(vinylpyridine), selected as a model compound, was studied to determine the optimum conditions for the strongest SERS signal. The Raman enhancement resulted from the plasmon coupling of silver nanoparticles to the underlying continuous film as well as the lateral plasmon coupling between the silver nanoparticles. The formation of the charge transfer complex was also observed. The 3S configuration was used to obtain SERS spectra of dipicolinic acid (DPA), a chemical signature for *Bacillus anthracis*.

Introduction

Raman spectroscopy is a powerful analytical technique that provides rapid and nondestructive analysis. The Raman technique gives highly specific information for the chemical analysis of compounds and can be used for multicomponent analysis. Raman scattering, however, is a low probability event, and conventional Raman spectroscopy is limited by its low sensitivity.[1] However, surface-enhanced Raman scattering (SERS) is able to overcome the limitations of conventional Raman spectroscopy. In the 1970s, it was discovered that the Raman scattering efficiency could be enhanced when a compound was brought near or adsorbed onto special metal surfaces.[2] Fleischmann et al.[3] reported the first measurement of a surface-enhanced Raman spectrum from pyridine adsorbed on an electrochemically roughened silver electrode in 1974. Similar studies that were done by Van Duyne and Jeanmaire[4] and also Albrecht and Creighton[5] demonstrated that Raman scattering from pyridine on a roughened silver electrode could be enhanced by at least 6 orders of magnitude.

Electromagnetic (EM) enhancement and chemical enhancement are two important mechanisms responsible for the enhancement found in SERS. The chemical enhancement results from specific interactions between the adsorbed molecules and the surface leading to increased polarizability of the complex (i.e., the formation of a charge transfer state).[6] This mechanism involves either (a) the shifting or broadening of the electronic states of the adsorbed molecules due to their interaction with the metal or (b) electronic coupling and the formation of charge transfer intermediates due to the close proximity of the metal and the adsorbed molecule. The chemical enhancement is not well understood, however, and its contribution to the total SERS signal cannot be separated from the contribution of electromagnetic enhancement.[7] The primary contribution to SERS enhancement is an enlargement of the local electromagnetic field, due to the excitation of a localized surface plasmon (electromagnetic enhancement).[8] The electromagnetic (EM) field enhancement stems from the roughness-induced excitation of surface-plasmon polaritons (SPPs) by the incoming light, resulting in large EM fields in the vicinity of the metal surface that strongly polarize the adsorbed molecules. A SPP can be either propagating along a continuous surface (extended SPP) or confined within metal particles (localized plasmon resonances).[1] Surface morphology with a roughness scale of ∼50−200 nm is crucial to exhibiting a large enhancement factor.[9] Surface roughness can be created in a number of ways such as oxidation−reduction cycles on electrode surfaces, adsorption of metal colloids onto the surfaces, vapor deposition of metals onto dielectric substrates, and metal nanostructures produced via lithography.[10] All of these methods produce small metal particles or aggregates of particles on the surface that are capable of providing the metal with the required roughness features needed for enhancement. When small metal particles are excited by light, plasmon modes are created and as a result near field regions around each particle are also created. These fields can couple to analyte molecules that are in close proximity and result in enhanced Raman scattering from the analyte molecules. Since the surface electrons of the metal are confined to the particle, the plasmon excitation is also confined and the resulting electromagnetic field of the plasmon is very intense.[11] For closely spaced nanoparticles, plasmon coupling takes place and the local field is concentrated in the space between the particles. It is widely accepted that the strongest SERS originates from the molecules that are placed between coupled plasmonic particles, for example, in aggregated metal colloids.[12] Such nanocrystal junctions can also lead to SERS via electron tunneling that takes place between two metal particles by means of exciting molecular vibrational modes.[13]

Surface structure on atomic and nanometer scales affects chemical and electromagnetic enhancement mechanisms, and much work has been done to fabricate substrates that produce greater enhancement. The first substrates to produce enhanced Raman signals and most commonly used substrates were electrochemically roughened Ag electrodes.[14,15] These surfaces were prepared by a series of oxidation−reduction cycles and produced protrusions in the range 25−500 nm. Since this early discovery, several methods for preparing SERS-active substrates have been investigated. Vapor-deposited Ag films are another type of commonly used SERS substrates. The physical vapor deposition process involves electrothermal evaporation of a

* To whom correspondence should be addressed. E-mail: gchumak@clemson.edu.

10.1021/jp053432a CCC: $30.25
Published on Web 09/03/2005

metal under high vacuum conditions. The evaporated particles aggregate at the surface of the substrate and form isolated islands. These substrates offer the advantage of having some control over the optical properties and the surface morphology of the film. Having control of these features directly affects the sensitivity of the SERS substrates.[14,16] Metal nanoparticles have received much attention as potentially useful materials for SERS substrates. The metal nanoparticles are adsorbed to the surface of the substrates to create roughness features depending on the size of the nanoparticle adsorbed. The particles are usually 10−100 nm in diameter and can be used as a dried solid or as an aqueous suspension. The optical and electronic properties of metal nanoparticles depend on the size, shape, and morphology of the nanoparticles, and these properties can be tuned to suit various applications. Another advantage of metal nanoparticles as substrates is their simplicity in preparation and ease of characterization.[11,17]

The complexity of the SERS phenomenon and the lack of models that are capable of predicting both the appearance of SERS spectra for a specific molecule and the magnitude of Raman enhancement necessitate the optimization of substrates for every compound under study. Here, we report the development of a sandwich SERS substrate (3S) that exploits the plasmon coupling between a single layer of silver nanoparticles and a smooth, continuous silver film with analyte molecules sandwiched in between. A relevant study was recently published using gold nanoparticles.[18] The main motivation is the development of a SERS substrate optimized for the detection and quantification of dipicolinic acid (DPA), which is a chemical signature of the genus *Bacillus* including *B. anthracis*.[19] In addition to DPA, poly(vinylpyridine) (PVP) was used as a model compound for substrate optimization because both molecules have the same pyridyl group which is known to produce strong SERS (reporter) and PVP is also a good coupling layer for the attachment of the nanoparticles to the substrate.

Experimental Section

Materials. Ag_2O (99.99%) was purchased from Alfa Aesar. Hydrogen gas (99.9999%) was purchased from National Welders Supply Company. Microscope glass slides were purchased from Fisher Scientific. Poly(4-vinylpyridine) (MW 40 000), polydiallyldimethylammonium chloride (MW <200 000), and 2,6-pyridinedicarboxylic acid (dipicolinic acid) were purchased from Aldrich. Reagent alcohol (HPLC grade) was purchased from Fisher Scientific. All chemicals were used as purchased with no further purification. Water with a nominal resistivity of 18 MΩ·cm was obtained from a Millipore Milli-Q system.

Synthesis of Ag Nanoparticles. Silver nanoparticles were synthesized by a hydrogen reduction reaction previously reported by this lab.[20] Briefly, an aqueous solution of saturated silver oxide was reduced with hydrogen gas. A special reaction vessel was used to synthesize the silver nanoparticles. The vessel was filled with 3 L of Milli-Q water, and 2 g of silver(I) oxide was added. To produce silver seeds, the vessel was shaken vigorously. A heating mantel was used to heat the vessel to the desired temperature. The solution was heated to 70 °C and exposed to hydrogen gas at 10 psi. Shortly after the vessel was pressurized, the solution color changed from clear to light yellow, indicating the formation of silver nanoparticles from the seeds present in the vessel. The reaction was monitored using UV−visible spectroscopy. Aliquots of the reaction mixture were taken in 15 min intervals. A total of five different sizes of silver nanoparticles were used in these experiments. The extinction spectra of the aliquots used for the 3S fabrication in these experiments are shown in Figure 1.

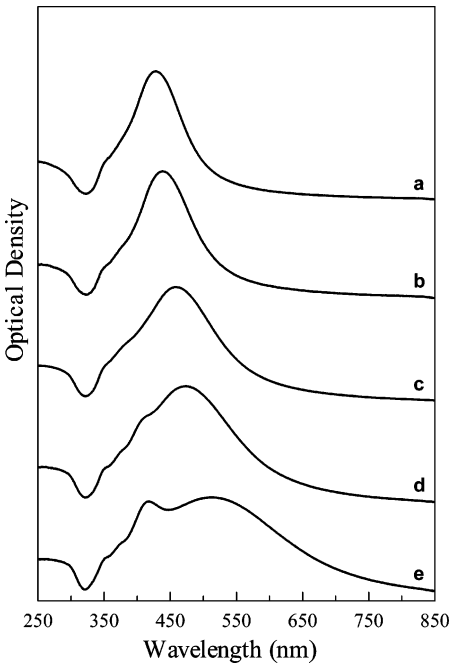

Figure 1. Extinction spectra of the five different sizes of Ag nanoparticles in water used to fabricate sandwich SERS substrates: (a) 28 nm; (b) 33 nm; (c) 50 nm; (d) 65 nm; (e) 100 nm.

Fabrication of Smooth Ag Mirror Films. Microscope slides were cut into 25 mm × 10 mm slides. The slides were first cleaned with soap and water and then placed into a 1:3 mixture of 30% H_2O_2/H_2SO_4 (piranha solution) for 30 min under continuous sonication. *Caution: Piranha solution is a very strong oxidizing agent and reacts violently with organic compounds. It should be handled with extreme care.* The slides were rinsed with Milli-Q water followed by drying under a stream of nitrogen and plasma cleaning for ∼1−2 min. The slides were then immersed in a 1% solution of poly(vinylpyridine) for several hours and, following thorough rinsing with reagent alcohol, were placed into an oven at 100 °C for 20 min. (Note that, for the fabrication of the Ag films, PVP was used as an adhesive to help the silver metal stick to the glass slides.)[21] The polymer modified slides were then placed in the vacuum deposition chamber. Continuous films were prepared by the thermal evaporation of bulk Ag metal at 10^{-6} Torr using an Edwards coating system (model E306A). The thickness of the films was not measured, since it was only important to obtain a smooth, continuous film and not metal islands. As the metal was deposited, the appearance of the films changed from clear to a slightly blue tint and finally to a shiny mirrorlike surface, indicating that a continuous film was obtained.

Fabrication and Characterization of Mirror Sandwich SERS Substrates (M3S). The Ag mirror films were further modified with two different polymers functioning as a coupling layer for Ag nanoparticles.[22] The films were exposed to 1% ethanolic PVP or 1% aqueous polydiallyldimethylammonium chloride (PDDA) solution overnight. After thorough rinsing in the pure solvents, the films were dried at 100 °C for approximately 2 h and placed into aqueous suspensions of different sized Ag nanoparticles. The exposure took place for 1 week to allow the saturation of the film surface with the nanoparticles. A total of five different particle diameters were used to make five different SERS-active substrates. The adsorption of nanoparticles to the substrates was monitored by UV−vis spectroscopy in the reflectance configuration. Reflectance spectra of the mirror sandwich SERS substrates (M3S) were collected using a Shimadzu UV-2501PC spectrometer. All spectra were pro-

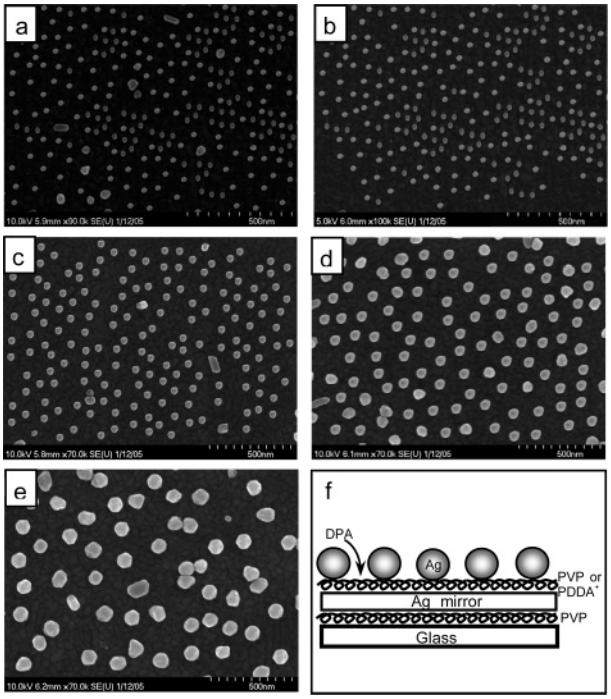

Figure 2. (a−e) Scanning electron microscope images of the five substrates used. (f) Schematic diagram of the sandwich SERS substrates.

cessed and figures prepared using Spectra-Solve for Windows (LasTek Pty. Ltd.). The films were then examined with a field emission scanning electron microscope (SEM) (Hitachi, S-4700) operating between 8 and 12 keV to determine the size distribution, shape, and aggregation state of the nanoparticles. The continuous Ag films provide the electrical conductivity required for SEM measurements. The characteristic SEM images of the five different substrates are shown in Figure 2. In addition to the smooth, continuous Ag films, electrochemically roughened Ag substrates were used for the electrochemical 3S (E3S). Roughening was performed in a standard three-electrode cell by passing ~25 μC/cm^2 at +0.5 V versus SCE to oxidize the continuous Ag film followed by the reduction of the metal at −0.65 V until the current reached its minimum.

SERS Measurements. The Raman instrument included a spectrograph (Triplemate 1377) interfaced to a liquid-nitrogen-cooled CCD detector (Princeton Instruments, model LN1152) and Innova 200 argon ion and Innova 100 krypton ion laser excitation sources. The SERS spectra were obtained by excitation with 457.9, 476.5, 488.0, 514.5, 530.9, 568.2, and 647.1 nm radiations. The laser power used was about 50 mW at the samples. The total acquisition time was 1.5 min for each sample. The scattered light was collected in a backscattering geometry with a 0.24 nm resolution. The Raman spectra were calibrated with indene.

Results and Discussion

The surface-enhanced Raman scattering spectrum of DPA on the mirror 3S (M3S) is shown in Figure 3 and compared to those measured on electrochemically roughened Ag substrates (SERS benchmark) and on the E3S. Electrochemical 3S were made by attaching 65 nm Ag particles to an electrochemically roughened Ag surface via PDDA. The polymer is positively charged and attracts DPA molecules into the region between the Ag nanoparticles and the continuous Ag film where the strongest localization of the local electromagnetic field is expected. By itself, the PDDA polymer yields only a weak SERS

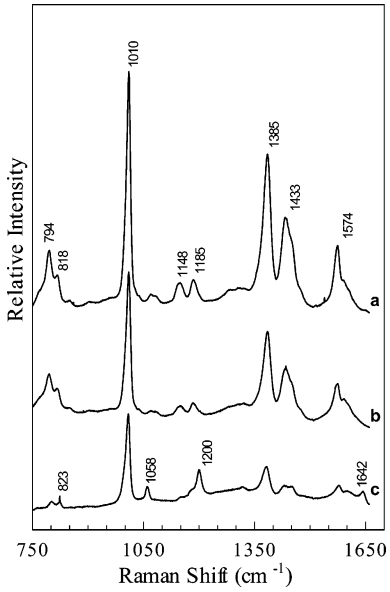

Figure 3. SERS spectra of DPA: (a) M3S; (b) E3S; (c) electrochemically roughened Ag surface. Excitation wavelength, 568.2 nm; power density, 7 W/cm^2; integration time, 100 s.

spectrum, which does not interfere with that of DPA. All three substrates yielded strong SERS spectra of DPA with the strongest signal coming from the M3S. Despite the similarity of all spectra, there are noticeable spectral differences between the electrochemically roughened Ag surface and the other two substrates. The differences can be attributed to the different interactions of DPA molecules with the SERS substrates and different contributions from the chemical and electromagnetic mechanisms of Raman enhancement. In the case of the electrochemically roughened surface, the pyridyl moiety most likely interacts directly with the silver surface through the lone electron pair on the nitrogen atom and the contribution from the chemical enhancement is significantly greater as compared with that of the electromagnetic enhancement. It is important to emphasize that when both mechanisms are present, the SERS spectra exhibit features characteristic for the chemical enhancement alone and usually result in SERS spectra that are different from those of molecules in their free state due to surface interactions. Contrary to the electrochemically roughened surface, the DPA molecules on the M3S interact electrostatically with the PDDA polymer and the enhancement originates from the enhanced local field in the space between the particles and the continuous film. Evidence of the latter can be seen from the fact that SERS spectra on M3S and E3S appear to be identical. Even though the underlying substrate of the E3S is an electrochemically roughened Ag surface, no spectral features characteristic of an electrochemically roughened surface can be seen. This observation implies that the direct interaction of DPA molecules with the silver does not occur in the M3S and, consequently, there is no chemical enhancement of Raman scattering on these substrates. Further development of the sandwich SERS substrates was performed using PVP as a model compound with the goal of optimizing the enhancement of Raman scattering.

Surface-enhanced Raman spectra of PVP were measured on an electrochemically roughened silver surface, M3S, and E3S (Figure 4). The major bands observed in the spectra from these substrates are the following: 680 cm^{-1} (in-plane ring deformation), 1005 cm^{-1} (ring breathing), 1204 cm^{-1} (C−C stretch between the ring and the polymer backbone), and 1613 cm^{-1} (ring stretching).[23−25] The overall signal intensity is largest on

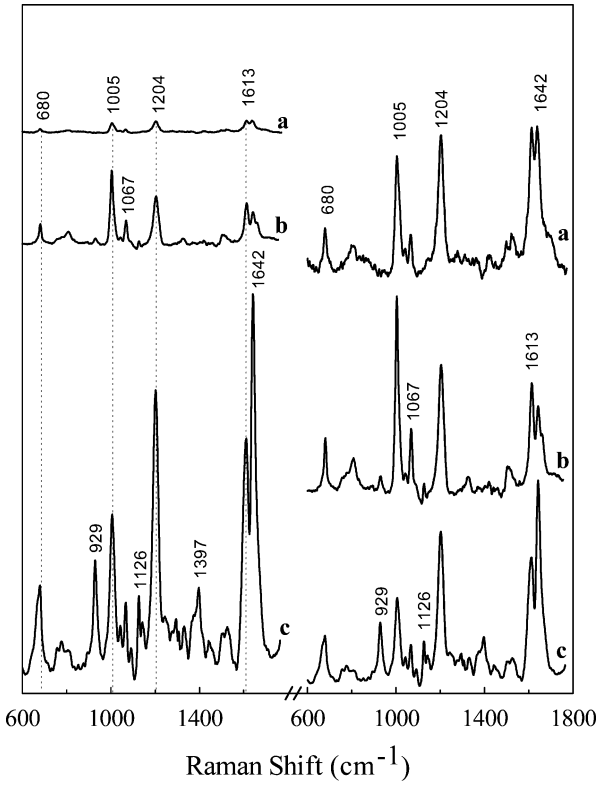

Figure 4. SERS spectra of PVP: (a) electrochemically roughened Ag surface; (b) E3S; (c) M3S. The spectra shown in the right panel are normalized to the 1204 cm^{-1} band. Excitation wavelength, 514.5 nm; power density, 7 W/cm^2; integration time, 100 s.

the M3S, followed by the E3S and then the electrochemically roughened Ag surface. The 20-fold SERS increase on the M3S as compared with the electrochemically roughened Ag surface clearly indicates the advantage of these new SERS substrates (Figure 4, left panel). However, there are differences between the spectra, namely, the appearance of new bands at 929, 1126, and 1397 cm^{-1} in the spectra of the M3S as well as changes in the relative intensities of other bands (Figure 4, right panel). The differences can result from three potential factors, the contributions of which could vary between the substrates. These factors include the following: (1) different degrees of electromagnetic and chemical enhancements, (2) the orientation of pyridyl groups relative to the metal surface, and (3) the number of pyridyl groups that interact with silver. The electromagnetic mechanism is due to the increased local electromagnetic field associated with plasmon resonances in silver nanostructures, and the chemical enhancement could result specifically from the resonant charge transfer interaction between the pyridyl groups and the metal. The relative contributions from the two mechanisms are a key factor, whereas the orientation of the pyridyl groups appears to be less important. The latter stems from the fact that the pyridyl groups in the polymer are randomly oriented and this random orientation removes the dependence of the SERS spectra on the orientation of the local field. For example, the local field in the M3S is in the direction normal to the substrate, but the field in the electrochemically roughened substrates is localized predominantly between nanosized metallic features and is in the plane parallel to the substrate. Assuming that Raman enhancement is solely due to the local field, randomly oriented molecules should yield the same SERS spectra in both cases. The third factor relates to the two different populations of the pyridyl groups present on the substrates: ones that interact with the metal surface and others that remain free. These two types of pyridyl groups could undergo different Raman enhancement and exhibit shifted vibrational frequencies as well as changes in the relative intensities of the bands.

The Raman scattering from the vibrations of the ring can undergo both electromagnetic and chemical enhancements, whereas the band at 1204 cm^{-1} from the C−C stretch is most likely enhanced by the local field. The contribution to the intensity of this band from the enhancement due to the charge transfer interaction is expected to be minimal because this bond is not conjugated to the pyridyl ring. For this reason, the C−C stretch was selected as an internal standard to which all SERS spectra were normalized (Figure 4, right panel).

SERS of PVP was previously studied on electrochemically roughened silver surfaces[23] and silver island films.[24,25] Although the reported spectra were similar, some discrepancies were observed and explained in terms of photodegradation and thermal degradation of the polymer under different experimental conditions as well as the hydration of the pyridyl ring in the electrolyte solution. In the present work, the spectra measured from electrochemically roughened Ag surfaces and E3S are similar to those from refs 23−25 but also contain some differences. Specifically, the doublet at 1613 cm^{-1}/1642 cm^{-1} is blue shifted to 1637 cm^{-1}/1672 cm^{-1} in ref 23 and is reduced to a single band at 1613 cm^{-1} in ref 24. The band at 1642 cm^{-1} is assigned to a photodegradation product of the polymer, and measuring SERS spectra with lower energy excitation photons further corroborated this assignment. As the excitation wavelength was increased from 514.5 to 530.8 nm and then to 568.0 nm, the band at 1613 cm^{-1} progressively disappeared.

Contrary to the SERS spectra of DPA, the spectrum of PVP obtained from the E3S is similar to that measured from the electrochemically roughened Ag surface. The E3S spectrum is also 5 times stronger, indicating that the SERS from the electrochemically roughened surface is further enhanced via an electromagnetic mechanism by adsorption of the Ag nanoparticles on top on the polymer. As mentioned above, DPA molecules interact with the SERS substrate differently for E3S and electrochemically roughened Ag surfaces, whereas in the case of PVP the polymer interacts in the same way with both substrates through the lone pair on the nitrogen atom of the pyridyl ring. Both chemical and electromagnetic enhancements contribute to the Raman signal in this system.

The SERS spectra of PVP from the M3S that have smooth, continuous Ag films instead of electrochemically roughened Ag surfaces contain more features as compared with the other two substrates. The most prominent band appeared at 929 cm^{-1} along with other features at 1091, 1126, and 1397 cm^{-1}. This observation is somewhat surprising, as smooth Ag films are not known to produce SERS and the interaction of Ag nanoparticles with the PVP coupling layer is not expected to be different from that in the case of E3S. SERS spectra with more features would be expected from E3S rather than from M3S because of the two different enhancement mechanisms that are clearly present in the case of electrochemical 3S: (1) the chemical enhancement from the electrochemically roughened surface and (2) the electromagnetic enhancement from the plasmon coupling between Ag nanoparticles and the underlying Ag surface. The two mechanisms enhance the Raman scattering of different populations of the pyridyl group: ones that directly interact with the surface and those that do not. These can potentially yield different vibrational spectra, producing overall richer SERS spectra. The new spectral features observed on the M3S originate from the plasmon coupling between Ag nanoparticles and the underlying substrate. Even though the nanoparticles that are used

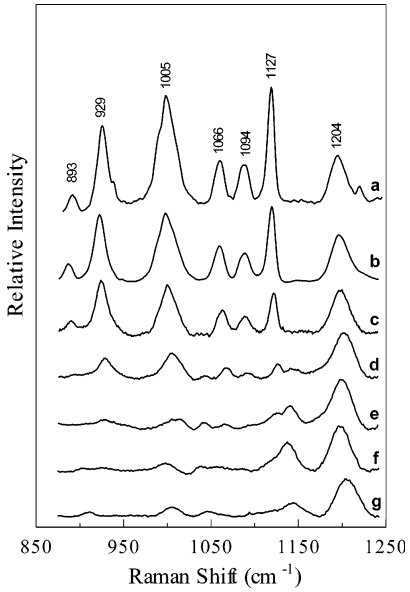

Figure 5. SERS of PVP on M3S fabricated with 65 nm Ag nanoparticles: (a) 647.1 nm; (b) 568.2 nm; (c) 530.9 nm; (d) 514.5 nm; (e) 488.0 nm; (f) 476.5 nm; (g) 457.9 nm (excitation wavelengths). Power density, 7 W/cm^2; integration time, 100 s.

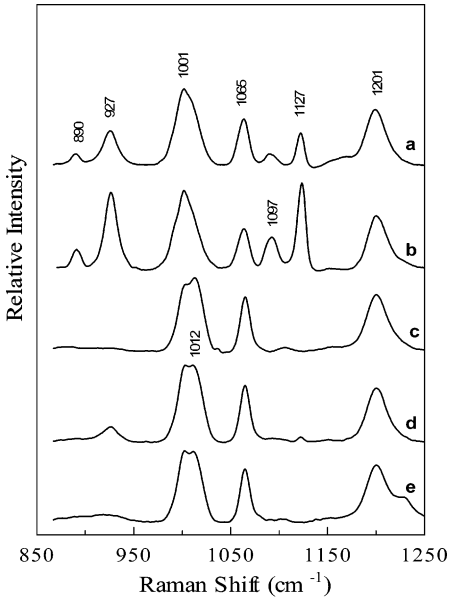

Figure 6. SERS spectra of PVP on M3S fabricated with different sizes of Ag nanoparticles: (a) 100 nm; (b) 65 nm; (c) 50 nm; (d) 33 nm; (e) 28 nm. Excitation wavelength, 568.2 nm; power density, 7 W/cm^2; integration time, 100 s.

in M3S and E3S are the same, the coupling is different in both systems because the two substrates support different plasmon modes.

It is hypothesized that the new bands observed from the M3S correspond to a charge transfer complex between the pyridyl rings of the polymer and the silver metal film. The band at 929 cm^{-1} appears to be the ring breathing mode that has downshifted from 1005 cm^{-1} due to the electron transfer that takes place from the ring to the metal, thus weakening the π electron system. The formation of this complex can be viewed as the (partial) oxidation of the ring by the oxide layer present on the silver particles, which is known to be a strong oxidizer. Whether this complex is formed in the dark or is photoinduced by light when exciting SERS will be addressed further. Some evidence of the complex formation can be found in Figure 4b in which a weak band at 929 cm^{-1} starts to appear on the E3S; however, the intensity of this peak depends on the electrochemical roughening procedure and varies between different preparations. It is well-known that the electrochemical roughening of Ag surfaces suffers from SERS irreproducibility, largely due to the lack of total control of the surface roughness on both atomic and nanosize scales. On the contrary, SERS spectra on M3S are always highly reproducible provided that the same procedure for their fabrication is followed and the same Ag nanoparticles are used.

The SERS excitation profile for PVP was measured for the M3S in order to further confirm the existence of the charge transfer complex. The intensity of bands corresponding to the vibrations of the pyridyl ring increased relative to that of 1204 cm^{-1}, as well as the appearance of new bands at 929, 1094, and 1127 cm^{-1} (previously assigned to the charge transfer complex) when the excitation wavelength was changed from the blue to the red spectral range (Figure 5). Sandwich SERS substrates on continuous Ag films were also fabricated with different sizes of Ag particles to study the resonance interaction of the photoinduced charge transfer with plasmon modes in the system. Various sizes of particles have plasmon resonances at different frequencies and, when coupled to the mirror, produce different sets of plasmon modes. SERS spectra of PVP measured from these M3S exhibit a strong dependence on the size of the particles in both the observed bands and the overall intensity at all excitation wavelengths, as exemplified in Figure 6 at a 568.2 nm excitation. All of the different sizes of Ag nanoparticles in these M3S were synthesized via the hydrogen reduction method, and aliquots were taken from the same reaction at different times as the particles grew in order to ensure that their surface chemical properties were identical. The only difference between the particles was their size and the frequency of the plasmon resonance.

The observed differences in the SERS spectra from the M3S with different sizes of Ag nanoparticles can be explained in terms of the plasmon coupling between the nanoparticles and the mirror. For plasmonic particles that are close to a conducting substrate and are irradiated with light, the oscillating electrons in the particles induce electron oscillations in the surface layer of the substrate, thus producing "images" of the plasmonic particles. The plasmon resonances in the particles couple to the images in the substrate, resulting in a new set of coupled plasmon modes. The frequency of the coupled plasmon modes is determined by the plasmon frequency of the particles because the optical response of the continuous silver film is independent of the frequency of light in the visible spectral range. As the plasmon resonance shifts to the red spectral range (with increasing Ag particle size), it couples to the silver mirror, producing coupled plasmon modes that are also red-shifted. The red-shifted, coupled plasmon modes better overlap with the photoinduced charge transfer between the pyridyl rings and silver, thereby resonantly enhancing the Raman scattering of the complex. This enhancement is evident from the increased intensity of the corresponding bands at 927, 1097, and 1127 cm^{-1} as the particles size increases (Figure 6). It is apparent from this figure that Ag nanoparticles with a diameter of ~65 nm are the optimum size for producing the strongest SERS from the M3S.

Reflectance spectra measured from the M3S fabricated with different particle sizes are shown in Figure 7. As the particle size increased, a new band appeared around 600 nm that was assigned to the plasmon modes associated with the coupling between the Ag nanoparticles and the continuous Ag film. These modes are characterized by the local field that is concentrated

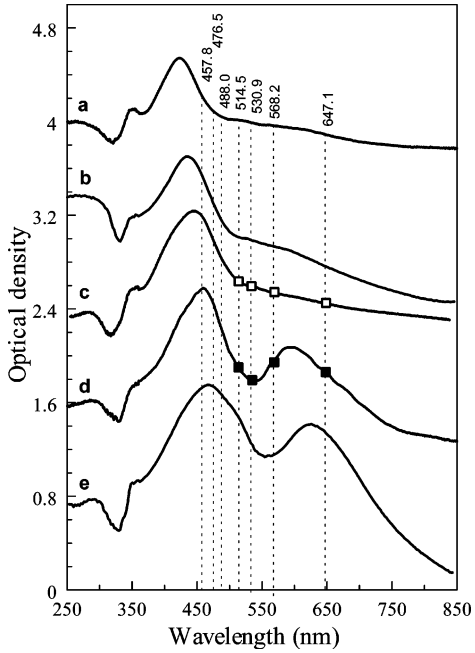

Figure 7. Reflectance spectra of M3S with different Ag nanoparticle sizes: (a) 28 nm; (b) 33 nm; (c) 50 nm; (d) 65 nm; (e) 100 nm. Open and closed squares indicate the excitation wavelengths used to excite SERS spectra in Figure 8.

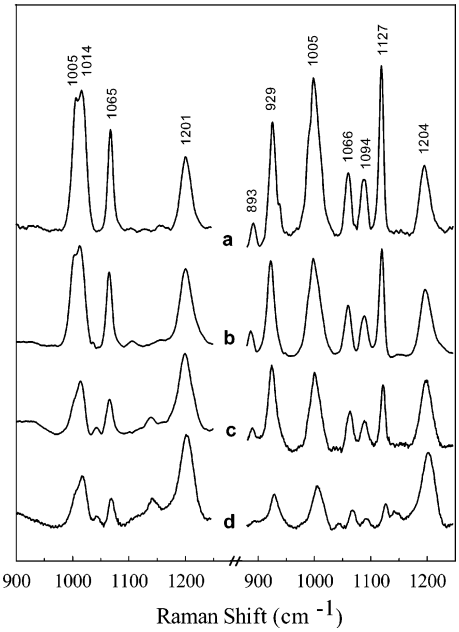

Figure 8. SERS spectra of PVP on M3S fabricated using two different sizes of Ag nanoparticles (right panel, 50 nm particles; left panel, 65 nm particles). Each substrate was measured at four excitation wavelengths: (a) 647.1 nm, (b) 568.2 nm, (c) 530.9 nm, and (d) 514.5 nm. Power density, 7 W/cm^2; integration time, 100 s.

in the space between the particles and the film leading to the enhancement of Raman scattering of molecules that are trapped in this space. In addition to this electromagnetic enhancement, there is a chemical enhancement due to the formation of the charge transfer complex, as was discussed above. An important question relating to the complex is whether it is formed in the dark or it is photoinduced. For the dark formation of the complex, its concentration remains the same and is independent of the excitation wavelength. In this case, the appearance of bands at 929, 1094, and 1127 cm^{-1} as the excitation wavelength shifts to the red spectral range (Figure 5) can be explained in terms of larger electromagnetic enhancement of Raman scattering due to the formation of the coupled plasmon modes. For the photoinduced formation of the complex, the trend in Figure 5 is due to both an increase in the complex concentration and larger electromagnetic enhancement, which occur with longer wavelength excitations. On the basis of the results in Figure 8, it was suggested that the formation of the charge transfer complex is photoinduced. In this figure, SERS spectra from two different M3S that have ∼50 nm (Figure 8, left panel) and ∼65 nm (Figure 8, right panel) Ag particles are compared at four excitation wavelengths: 647.1 nm (a), 568.2 nm (b), 530.9 nm (c), and 514.5 nm (d). (Note that the excitation wavelengths and their relevance to the M3S reflection spectra are depicted in Figure 7 as open and solid squares.) Whereas the M3S with larger particles clearly show the bands characteristic of the complex when excited with the selected wavelengths (right panel), there is no evidence of these bands from the M3S with smaller particles at any excitation wavelength (left panel). If the charge transfer complex forms in the dark, one would also expect to observe its characteristic SERS bands from the M3S with smaller particles when the appropriate excitation is used. It is important to note that the smaller particle M3S yielded similar SERS spectra to those shown in Figure 8 (left panel) with other excitation wavelengths (457.9, 476.5, and 488.0 nm) used in this study, while the spectra from the larger particle M3S exhibited the same trend for which the characteristic bands of the complex progressively decreased with the excitation wavelength shifting to the blue spectral range. Because the complex is formed under irradiation with light that is resonant with the coupled plasmon modes, it is called a plasmon assisted, photoinduced charge transfer complex. The electron transfer in this complex takes place from the pyridyl groups of PVP to the silver metal as discussed above; however, it is difficult to determine at this point whether the electrons are transferred to the particles or to the continuous film.

There is a dramatic change in the reflectance spectra (Figure 7) and corresponding SERS spectra measured from the M3S that have ∼50 nm Ag particles and those that have ∼65 nm Ag particles (Figure 8); however, UV−vis spectra of these particles in suspension exhibit only gradual changes (Figure 1c and d). Considering that the diameters of the Ag particles only vary by 15 nm, it is unlikely that such a dramatic change is solely due to the differences in coupling of the two different sizes of Ag particles to the silver mirror. We suggest the presence of an additional coupling, specifically, the plasmon coupling between individual particles. Such two-dimensional, "lateral" coupling was previously described and shown to be very sensitive to the interparticle distance as well as the size of the particles; hence, smaller particles would require much closer distances for plasmon coupling to take place.[26] The dependence on the interparticle distance is so sharp that it required only a 50% increase from the distance that produces the maximum coupling to completely decouple the system. It is believed that, under the conditions used here to fabricate M3S, substrates fabricated using particles with diameters of 50 nm and smaller did not experience lateral coupling, whereas larger particles did. The red band observed in the reflectance spectra of the M3S fabricated with larger particles corresponds to modes resulting from the plasmon coupling between the particles themselves and to the underlying continuous Ag film.

To determine the optimum size of Ag nanoparticles and the excitation wavelength that leads to the largest Raman enhancement, the SERS excitation profile was measured for M3S fabricated using different sizes of Ag particles. The M3S were placed into a plastic cuvette used for UV−vis spectroscopy

(Fisher Scientific) and pressed against the front window through which excitation and collection of Raman scattering took place. In addition to SERS spectra from M3S, Raman bands from the cell were simultaneously recorded and used as an external standard for SERS normalization. The SERS intensity was also normalized per density of Ag particles on the continuous films in order to expose the particle size dependence. As was expected on the basis of Figure 4, the strongest SERS signal was obtained at different excitation wavelengths depending on the size of the Ag nanoparticles used for M3S. A good correlation was made as to how well the excitation wavelength overlapped with the plasmon resonance of M3S, so that the better the overlap, the stronger the SERS signal observed. However, the yielded SERS spectra were different depending on whether SERS was excited in the blue or red plasmon band. The overall largest enhancement was obtained from the M3S fabricated using 65 nm Ag particles on continuous silver films and excited with 568.2 nm radiation.

In conclusion, immobilization of Ag nanoparticles on continuous Ag films results in highly reproducible sandwich substrates capable of enhancing the Raman scattering of molecules. The Raman enhancement originates from the enhanced local electromagnetic field associated with plasmon modes produced by plasmon coupling between the particles themselves as well as coupling between the particles and the underlying continuous film. The enhanced local field can initiate photochemical reactions as was observed in this study with PVP molecules. The coupling can be controlled by changing the distance between the particles and the film as well as the surface concentration of the particles and their size. This approach can lead to a general strategy for designing optimum SERS substrates. The M3S can be optimized for the largest Raman enhancement and a specific excitation wavelength by varying the size of the nanoparticles and potentially the interparticle distance. Substrates fabricated by this method have the advantage of utilizing the optical properties of metal nanoparticles but without the problem of SERS irreproducibility associated with the aggregation of the nanoparticles in colloidal suspensions. Additionally, with the proper selection of the polymer used to attach Ag nanoparticles to the continuous films, chemical selectivity for different analytes can be achieved, as was demonstrated here for dipicolinic acid.

Acknowledgment. We gratefully acknowledge the support of this work through Environmental Protection Agency, grant GR829603. We also acknowledge the Clemson University Center for Optical Materials Science and Engineering Technologies (COMSET) for continuous support.

References and Notes

(1) Moskovits, M. *Rev. Mod. Phys.* **1985**, *57*, 783.
(2) Otto, A.; Mrozek, I.; Grabhorn, H.; Akeman, W. *J. Phys. Chem.: Condens. Matter* **1992**, *4*, 1143.
(3) Fleischman, M.; Hendra, P. J.; Mcquillan, A. *Chem. Phys. Lett.* **1974**, *26*, 163.
(4) Jeanmaire, D. J.; Van Duyne, R. P. *J. Electroanal. Chem.* **1977**, *84*, 1.
(5) Albrect, M. G.; Creighton, J. A. *J. Am. Chem. Soc.* **1977**, *99*, 5215.
(6) Moskovits, M.; DiLella, D. P. In *Surface-Enhanced Raman Scattering*; Chang, R. K., Furtak, T. E., Eds.; Plenum Press: New York, 1982; p 243.
(7) Jiang, J.; Bosnick, K.; Maillard, M.; Brus, L. *J. Phys. Chem. B* **2003**, *107*, 9964.
(8) Campion, A.; Kambhampati, P. *Chem. Soc. Rev.* **1998**, *27*, 241.
(9) Schatz, G. C. *Acc. Chem. Res.* **1984**, *17*, 370.
(10) Chumanov, G.; Sokolov, K.; Gregory, B. W.; Cotton, T. M. *J. Phys. Chem.* **1995**, *99*, 9466.
(11) Kelly, K. L.; Coronado, E.; Zhao, L. L.; Schatz, G. C. *J. Phys. Chem. B* **2003**, *107*, 668.
(12) Gunnarsson, L.; Bjerneld, E. J.; Xu, H.; Petronis, S.; Kasemo, B.; Kall, M. *Appl. Phys. Lett.* **2001**, *78*, 802.
(13) Michaels, A. M.; Jiang, J.; Brus, L. *J. Phys. Chem. B* **2000**, *104*, 11971.
(14) Norrod, K. L.; Sudnik, L. M.; Roussell, D.; Rowlen, K. L. *Appl. Spectrosc.* **1997**, *51*, 994.
(15) Watanabe, T.; Maeda, H. *J. Phys. Chem.* **1989**, *93*, 3258.
(16) Van Duyne, R. P.; Hulteen, J. C.; Treichel, D. A. *J. Chem. Phys.* **1993**, *99*, 2101.
(17) El-Sayed, M. A. *Acc. Chem. Res.* **2001**, *34*, 257.
(18) Orendorff, C. J.; Gole, A.; Sau, T. K.; Murphy, C. *Anal. Chem* **2005**, *77*, 3261.
(19) Zhang, X.; Young, M. A.; Lyandres, O.; Van Duyne, R. P. *J. Am. Chem. Soc.* **2005**, *127*, 4484.
(20) Evanoff, D. D.; Chumanov, G. *J. Phys. Chem. B* **2004**, *108*, 13948.
(21) Malynych, S.; Luzinov, I.; Chumanov, G. *J. Phys. Chem. B* **2002**, *106*, 1280.
(22) Zheng, J.; Li, X.; Gu, R.; Lu, T. *J. Phys. Chem. B* **2002**, *106*, 1019.
(23) Garrell, R. L.; Beer, K. D. *Langmuir* **1989**, *5*, 452.
(24) Roth, P. G.; Boerio, F. J. *J. Polym. Sci., Part B: Polym. Phys.* **1987**, *25*, 1923.
(25) Venkatachalam, R. S.; Boerio, F. J.; Roth, P. G.; Tsai, W. H. *J. Polym. Sci., Part B: Polym. Phys.* **1988**, *26*, 2447.
(26) Malynych, S.; Chumanov, G. *J. Am. Chem. Soc.* **2003**, *125*, 2896.